J Forensic Sci, November 2006, Vol. 51, No. 6
doi:10.1111/j.1556-4029.2006.00266.x
Available online at: www.blackwell-synergy.com

Cedric Neumann,[1] M.Sc.; Christophe Champod,[2] Ph.D.; Roberto Puch-Solis,[1] Ph.D.; Nicole Egli,[2] M.Sc.; Alexandre Anthonioz,[2] M.Sc.; Didier Meuwly,[1] Ph.D.; and Andie Bromage-Griffiths[1], Bs.C.

Computation of Likelihood Ratios in Fingerprint Identification for Configurations of Three Minutiæ

ABSTRACT: Recent challenges to fingerprint evidence have brought forward the need for peer-reviewed scientific publications to support the evidential value assessment of fingerprint. This paper proposes some research directions to gather statistical knowledge of the within-source and between-sources variability of configurations of three minutiæ on fingermarks and fingerprints. This paper proposes the use of the likelihood ratio (LR) approach to assess the value of fingerprint evidence. The model explores the statistical contribution of configurations of three minutiae using Tippett plots and related measures to assess the quality of the system. Features vectors used for statistical analysis have been obtained following a preprocessing step based on Gabor filtering and image processing to extract minutia position, type, and direction. Spatial relationships have been coded using Delaunay triangulation. The metric, used to assess similarity between two feature vectors is based on an Euclidean distance measure. The within-source variability has been estimated using a sample of 216 fingerprints from four fingers (two donors). Between-sources variability takes advantage of a database of 818 ulnar loops from randomly selected males. The results show that the data-driven approach adopted here is robust. The magnitude of LRs obtained under the prosecution and defense propositions stresses upon the major evidential contribution that small portions of fingermark, containing three minutiæ, can provide regardless of its position on the general pattern.

KEYWORDS: forensic science, fingermark, fingerprint, identification, individualization, likelihood ratio, statistics

Recent challenges of fingerprint evidence (1–6) combined with recent cases of false identification (7–9) have strengthened the need for statistical research to underpin the fingerprint identification process. High priority has been given to such statistical research by a recent FBI committee charged with the review of the scientific basis for friction ridge skin comparisons as a means of identification (10).

A review of past statistical research in the fingerprint area has been recently published (11). Most of the research effort has been concentrated on level II features, namely minutia configurations. The term "minutiæ" refers to major ridge path deviations, also known as points of identification, or Galton details/characteristics. The two basic forms generally considered are ridge endings and bifurcations.

The most extensive forensic published studies to date have been carried out on a sample of around 1000 fingerprints from distinct individuals (12–14). These studies on minutiæ provide valuable knowledge, but they cannot yet be deployed for large-scale, case-specific calculations. As highlighted by Stoney, (15) none of the proposed models have been subjected to extended empirical validation studies. Indeed, the studies undertaken up to this point in time do not provide a robust tool for assessing the evidential value associated with all configurations of features on all fingers and for all general patterns. This is because:

- the previous models used do not fully capture the spatial relationship between minutiæ;
- the independence assumptions at the core of each model have not been fully tested;
- the studies focused on the estimation of a match probability with a weak account for tolerances due to distortion or clarity of the marks, including connective ambiguities;
- the effect of other variables such as general pattern, finger number, sex, or ethnic origin of the source has rarely been addressed; and
- none of the proposed models have been subjected to an extended empirical validation.

The present research is trying to address some of these limitations through the development of a model that will:

- capture the spatial relationship between minutiæ by using Delaunay triangulation;
- consider the variability of marks left by the same finger due to distortion;
- not require any independence assumptions;
- explore the effect of positioning of the configuration on the fingerprint surface and general pattern; and
- express the weight of evidence using a likelihood ratio (LR) that weighs together both the within-finger variability and the between-finger variability.

Our purpose is not to demonstrate the individuality of a complete and well-reproduced fingerprint, but to assess the evidential contribution of fingermarks that can be partial, distorted, and with a poor signal/noise ratio. To this end, we propose to explore here configurations of three minutiæ. A hypothetical case example will be used to illustrate the results that have been obtained.

[1]The Forensic Science Service, Trident Court, Birmingham Business Park, Birmingham B37 7YN, U.K.
[2]Ecole des Sciences Criminelles, Institut de Police Scientifique, Batochime, Quartier Sorge Université de Lausanne, CH-1015 Lausanne-Dorigny, Switzerland.

Received 8 July 2005; and in revised form 3 Feb. 2006; accepted 6 Feb. 2006; published 30 Oct. 2006.

Case Example

A partial fingermark is recovered from a crime scene. This fingermark (hereinafter the mark) contains an area where a neigh-

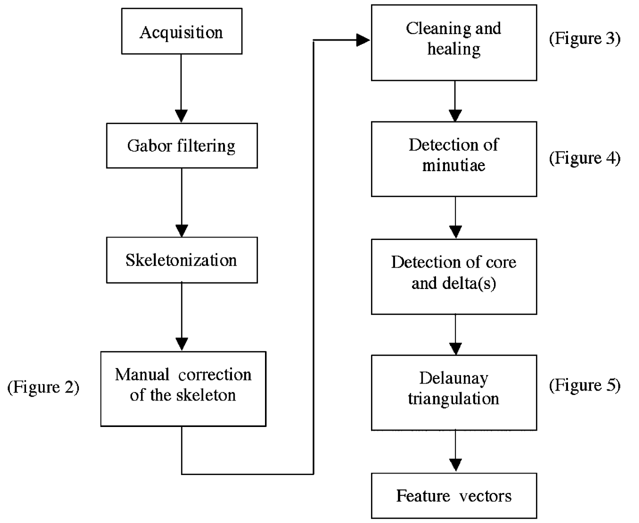

FIG. 1—*Flow chart of the preprocessing and feature extraction steps from acquired fingerprint images to a set of feature vectors.*

borhood of three minutiæ is clearly visible and partial information from which the general pattern and the region where the three minutiæ are can be inferred. A potential donor—Mr. X—has been the focus of the investigation and his fingerprints have been taken. One of Mr. X's fingerprints (hereinafter the print) shows the same general pattern as the fingermark, combined with three minutiæ of the same type, similar direction, and similar spatial arrangement.

Concept of a Likelihood Ratio for Fingerprint Evidence

A likelihood ratio (LR) is a statistical measure that offers a balanced presentation of the strength of the evidence (16). It is especially suitable for assessing the contribution of forensic findings (17,18). Stoney (19) proposed the use of an LR in his dissertation that has recently been applied in the field of marks and impressions (20–22). Formally, the LR is defined as follows:

$$LR = \frac{\Pr(E|S,I)}{\Pr(E|\bar{S},I)}$$

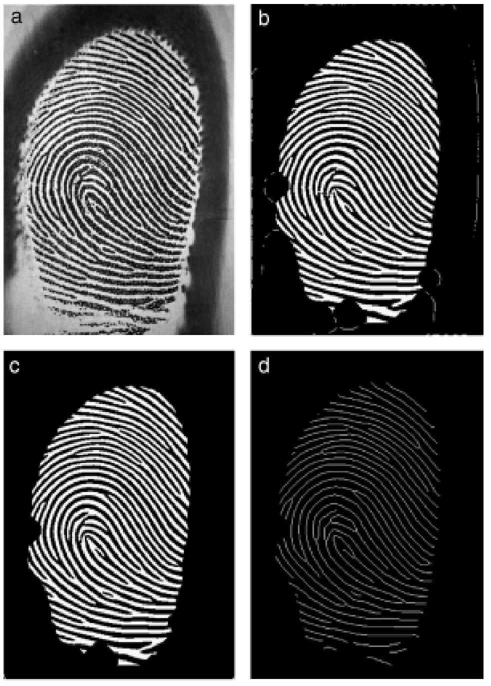

FIG. 2—*(a) Acquired image, (b) binary image obtained after Gabor filtering, (c) binary image manually corrected, and (d) corresponding skeleton.*

Where,

- E is the result of the comparison between the mark and the designated print from Mr. X;
- S is the hypothesis that Mr. X's designated finger has actually left the mark;
- (SPECIALS WITH THE BAR ON TOP) is the hypothesis that someone else, from a population of potential suspects, has left the mark; and
- I is the relevant background information the case, such as information on the selectioin of Mr. X and on the unknown source of the mark.

of the comparison between the *mark* and the designated *print* from Mr. X, *S* the Mr. X's designated *finger* has actually left the *mark*, $\bar{S}$ the someone else, from a population of potential

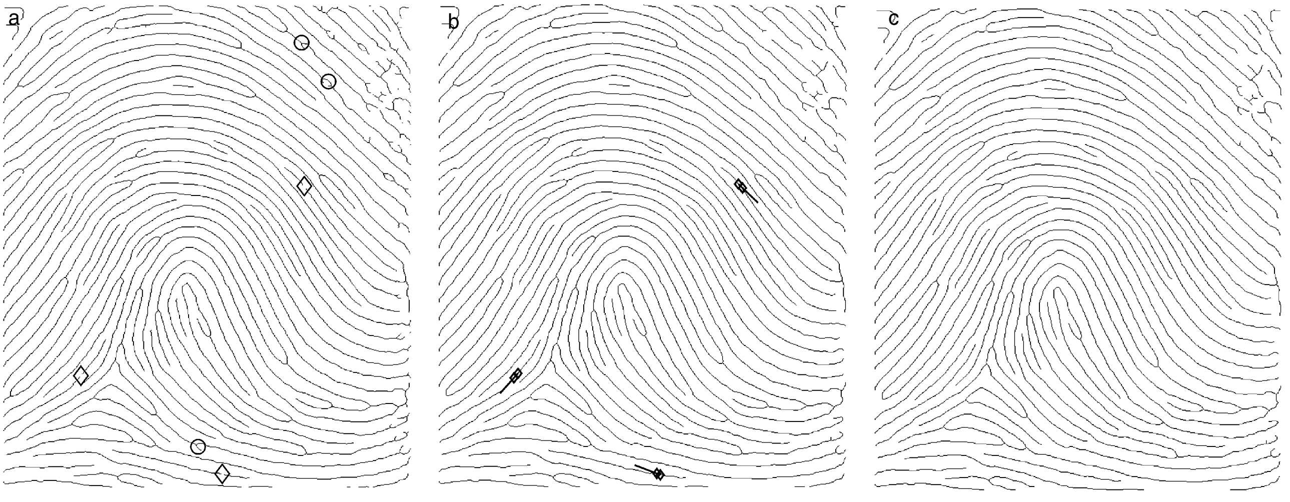

FIG. 3—*(a) Raw skeleton with the indication of spurs (circles) and ridge breaks (diamonds). (b) Spurs have been removed, ridge breaks are still indicated. (c) Skeleton obtained after removal of both spurs and ridge breaks.*

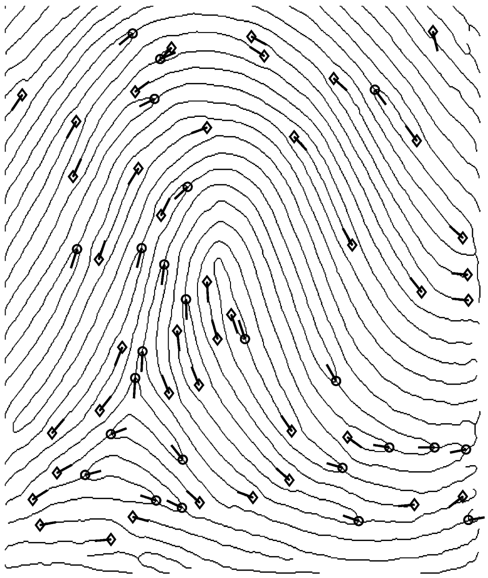

FIG. 4—*Skeleton with indication of ridge endings (in red) and bifurcations (in blue).*

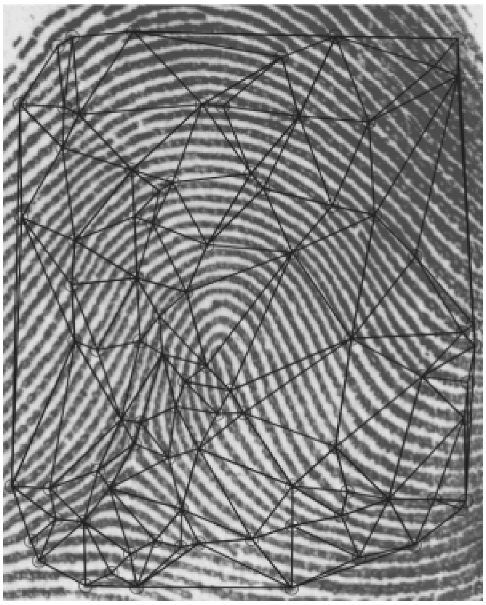

FIG. 5—*Delaunay triangulation superimposed on the original grayscale image.*

suspects, has left the *mark*, I the relevant background information on the case such as information on the selection of Mr. X and on the unknown source of the *mark*.

In the area of fingerprint evidence interpretation, the impact of I on the probabilities of the results is generally nonexistent. However, for the sake of generality, it will be retained in our development.

E in the above equation can be decomposed into y, the observation made on the *mark* and x, the observations made on the *print*. Hence, we obtain:

$$LR = \frac{\Pr(x, y|S, I)}{\Pr(x, y|\bar{S}, I)}$$

S implies that the considered minutia configuration on the mark not only comes from the suspect, but from a precisely defined minutia configuration on one of his fingers (i.e., the general pattern and the region of the suspect's finger are known). The following discussion is based on the aforementioned hypotheses. A change of hypotheses implies a different analysis.

The aim of the project is to assess LRs for configurations of three minutiæ. The numerator of the LR calls for an estimation of the density of the within variability of the features (same finger), whereas the denominator of the LR calls for an estimation of the

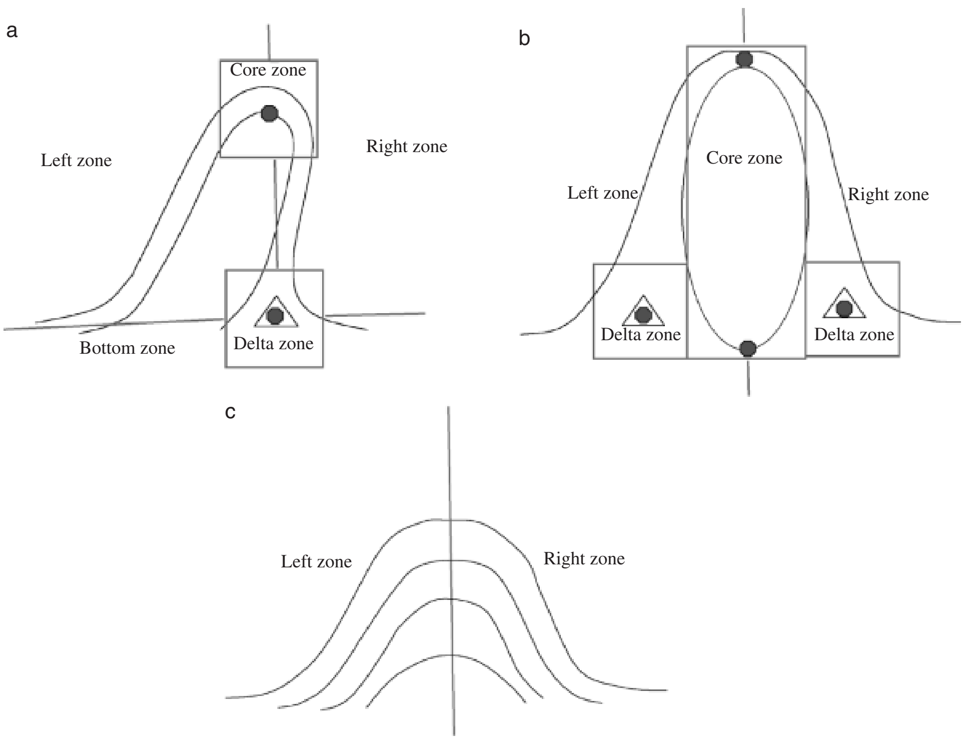

FIG. 6—*Illustration of the zones for, respectively, loops (a), whorls (b), and arches (c).*

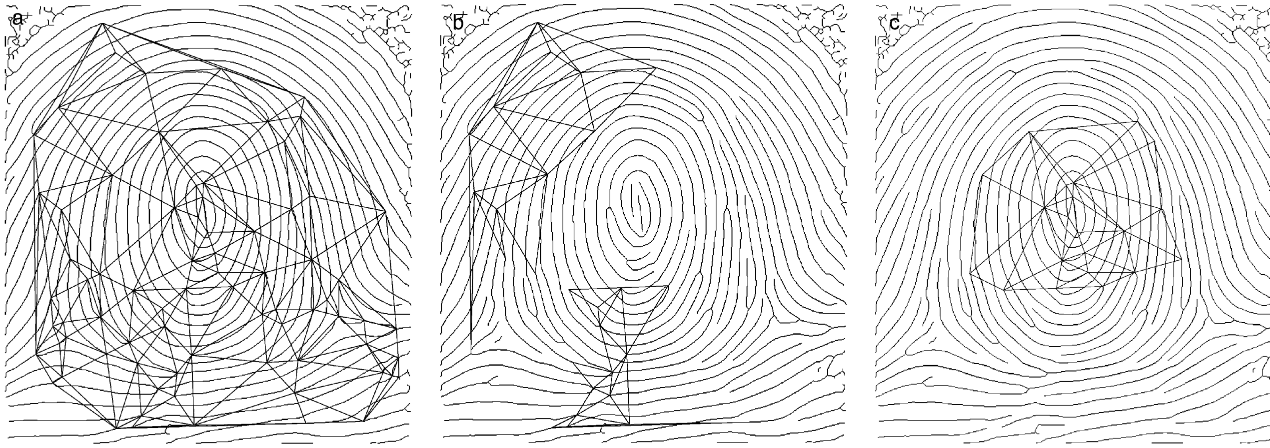

FIG. 7—*(a) Skeleton with Delaunay triangulation on all minutiae; (b) the triangles in the delta zone; (c) the triangles in the core zone.*

density of the between variability of the features (different fingers). These two assessments will be based on samples of known origin.

To assess the quality of this LR-based system, we will use Tippett plots (23–26). Tippett plots allow to compare the general magnitude of the LRs that we can expect from our methods under the two considered hypotheses of common source and of different sources. They allow to assess the discriminative power of the system and the rates of misleading evidence of the system.

Preprocessing and Feature Extraction

Images acquired to investigate the numerator and denominator of the LR have been processed (fully or partly) according to the flow chart in Fig. 1.

The images acquired for within variability were resized to a 1:1 scale at 500 dpi, treated using Gabor filtering (27,28)—programmed in Matlab®—and skeletonized after a manual check (and manual correction if needed) of the adequacy between the binary image and the initial grayscale image. An example is presented in Fig. 2.

Minutiæ, coded including a distinction between ridge endings and bifurcations, were automatically extracted from the skeletons of the images, followed by a step of cleaning and healing to remove artifacts arising from the skeletonization step such as spurs and broken ridges as shown in Figs. 3 and 4.

At this point, we obtained clean skeletons for both the within and the between-variability images. Features of statistical interest will be extracted from them taking advantage of Delaunay triangulation applied on the extracted minutiæ (29,30). In Fig. 5, an example of a fingerprint with the superposition of the triangulation of minutiæ is presented.

Previous research has shown the importance of taking into account the positioning on the papillary surface to assess the statistical significance of minutiæ (13). To investigate this, zones have been defined in relation to singular points (i.e., core and delta points). *Core* and *delta* points were extracted using the orientation field of the ridges according to the method described in Cappelli et al. (31), and general patterns and regions were defined using these singular points. One core and two deltas define a whorl, and one delta and one core define a loop. For whorls, the core, left and right delta, and left and right periphery were defined. For loops, only one delta, the core, and the left and right periphery are defined. The delta and core regions are circular, their diameter being half of the distance between the core and the delta. Right and left regions for whorls are defined by an axis passing through the core and the mean point of an axis between the two deltas, whereas for loops left and right are defined with respect to the line that can be drawn between the core and the delta. For arches, points of maximal curvature were used to establish a central axis and a left and a right zone were defined. Figure 6 illustrates the definition of the zones.

These defined zones allow the extraction of Delaunay triangles within predefined zones as illustrated in Fig. 7 for a whorl.

Using Delaunay triangulation, each fingerprint can be viewed as a collection of triangles. Each triangle can be described by a feature vector defined as follows: for the *print*, the feature vector is denoted x, and for the mark the feature vector is denoted y. Data extracted for each minutia—numbered 1–3—of the triangle are given between curly brackets.

$$
\begin{aligned}
x &= \left[GP_x, R_x, Rs, \{T_{2x}, A_{2x}, L_{2x-3x}\}, \{T_{3x}, A_{3x}, L_{3x-1x}\}\right] \\
y &= \left[GP_y, R_y, \{T_{1y}, A_{1y}, L_{1y-2y}\}, \{T_{2y}, A_{2y}, L_{2y-3y}\}, \right. \\
&\quad \left. \{T_{3y}, A_{3y}, L_{3y-1y}\}\right]
\end{aligned}
$$

where GP is the general pattern of the fingerprint (for this study all fingerprints are right loops), R is the zone from which the triangle originates (center, delta, right, and left periphery), T is the type of the minutia considered; T_{1x} is therefore the type of the first minutia from the triangle originating on the print. T can take a value of 1 for ridge ending and 2 for bifurcation, A is the direction (between 0 and 2π) of the minutia relative to the opposite side of the triangle, A_{1x} is the direction of the first minutia from the triangle originating from the print, L is the length in pixels of the side of the triangle, L_{1x-2x} linking minutia 1 and 2 of the triangle from the print.

We rearranged the feature vector to separate the *discrete* quantities (*GP, R, T*) from the *continuous* quantities (*A, L*) and we introduced a summary variable *Nt* combining the three types (*T*) giving the total count of ridge endings (*Nt* then takes four possible values [0, 1, 2, 3]). Hence, for x and y, respectively, we obtain the following feature vectors:

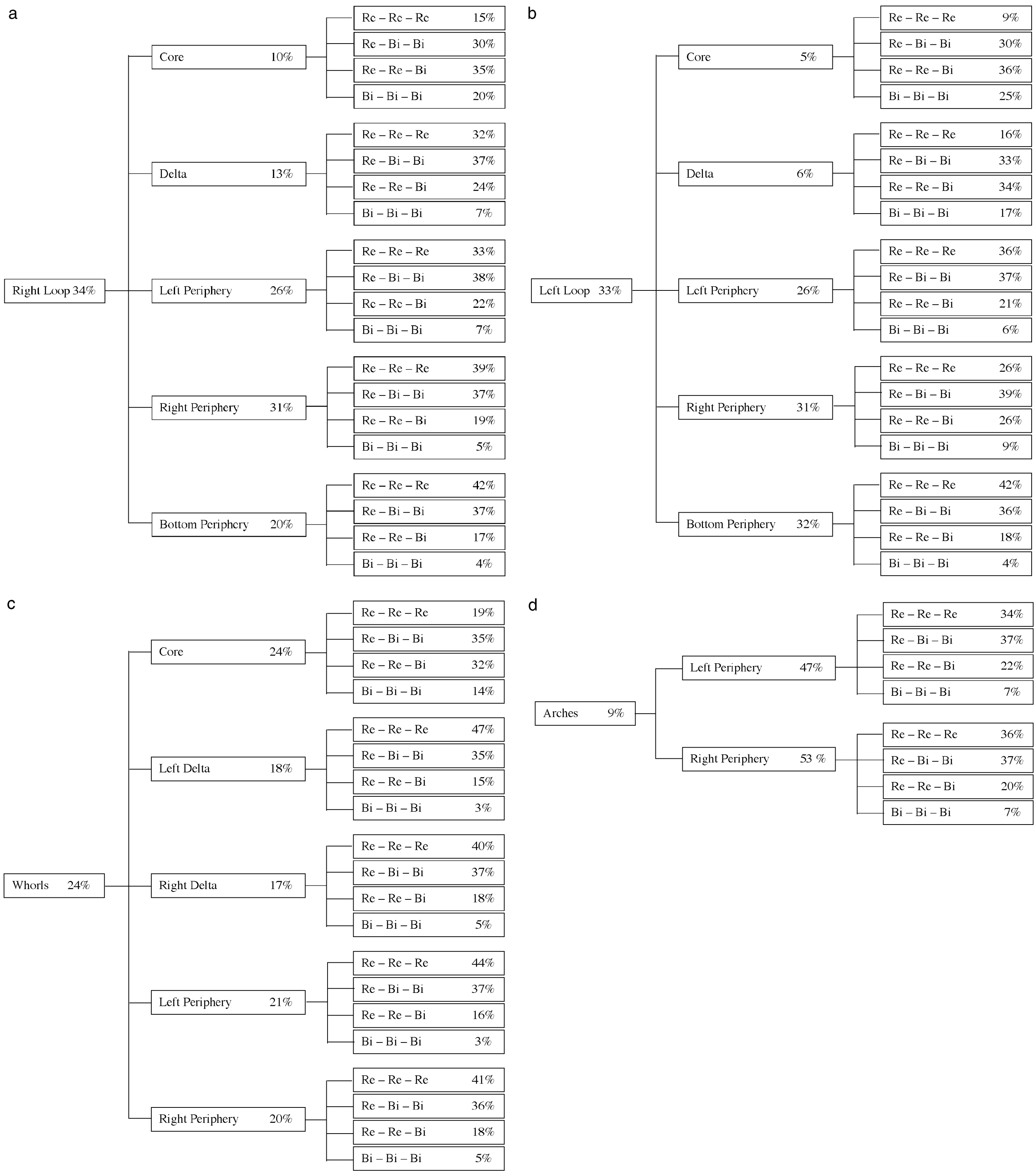

FIG. 8—*Probability tree used to compute the denominator of LR_d. Right loops (a), left loops (b), whorls (c), arches (d).*

$$x = [GP_x, R_x, Nt_x, \{A_{1x}, L_{1x-2x}\}, \{A_{2x}, L_{2x-3x}\}, \{A_{3x}, L_{3x-1x}\}]$$
$$x_{\text{discrete}} = [GP_x, R_x, Nt_x];$$
$$x_{\text{continuous}} = [\{A_{1x}, L_{1x-2x}\}, \{A_{2x}, L_{2x-3x}\}, \{A_{3x}, L_{3x-1x}\}]$$

Hence $x = [x_{\text{discrete}}, x_{\text{continuous}}]$ or for short $x = [x_d, x_c]$

$$y = \left[GP_y, R_y, Nt_y, \left\{A_{1y}, L_{1y-2y}\right\}, \left\{A_{2y}, L_{2y-3y}\right\}, \left\{A_{3y}, L_{3y-1y}\right\}\right]$$
$$y_{\text{discrete}} = \left[GP_y, R_y, Nt_y\right]; y_{\text{continuous}} = \left[\left\{A_{1y}, L_{1y-2y}\right\}, \left\{A_{2y}, L_{2y-3y}\right\}, \left\{A_{3y}, L_{3y-1y}\right\}\right]$$

Hence, $y = [y_{\text{discrete}}, y_{\text{continuous}}]$ or for short $y = [y_d, y_c]$

FIG. 9—*Images of the same finger under four different distortion states.*

Statistical Analysis

The purpose of the research is to assess LRs associated with comparison between a three-minutia mark and a corresponding arrangement on a print. Formally we can write:

$$LR = \frac{p(x,y|S,I)}{p(x,y|\bar{S},I)} = \frac{p(x_d,y_d,x_c,y_c|S,I)}{p(x_d,y_d,x_c,y_c|\bar{S},I)}$$

$$LR = \underbrace{\frac{p(x_c,y_c|x_d,y_d,S,I)}{p(x_c,y_c|x_d,y_d,\bar{S},I)}}_{LR_{c|d}} \underbrace{\frac{p(x_d,y_d|S,I)}{p(x_d,y_d|\bar{S},I)}}_{LR_d} = LR_{c|d} \cdot LR_d$$

The LR is expressed as a product of two LRs. The second ratio, LR_d, is the weight of the discrete variables, whereas the first ratio, $LR_{c|d}$, is the weight of the continuous variable (conditional on the discrete observations).

For LR_d, the value of the numerator is set to 1 because it is assumed that if two feature vectors are of the same source, there are no doubts on the fact that they originate from the same region of the same general pattern and that they code the same minutia types. This numerator will be investigated further in future work as there are some notable issues on the clarity of minutia types. The value of the denominator of the second term is the probability that two feature vectors originate from the same region of fingerprints having the same general pattern and that they have the same minutia-type combination. This probability is computed according to the probability tree shown in Fig. 8. The frequencies for general patterns are based on values compiled by the FBI for the National Crime Information Center in 1993 (http://home.att.net/ ~ dermatoglyphics/mfre/). Frequencies for the occurrence of the different regions for each general pattern and for the occurrence of each of the minutia-type combination for each region are based on the set of fingerprints used for the between variability. The denominator probability of being in a specific leaf of the tree is obtained by multiplying the frequencies of the branches.

TABLE 1—*Distribution of general patterns and ridge counts in the set of fingerprints used to assess between-finger variability.*

Description	Number
Ulnar loops from right index finger, ridge count 3–6	217
Ulnar loops from right index finger, ridge count 12–16	104
Ulnar loops from right middle finger, ridge count 3–6	185
Ulnar loops from right middle finger, ridge count 12–16	180
Total for dataset 1	*686*

To compute $LR_{c|d}$, an approach called the "data-driven" approach has been adopted. This approach is based on the two-by-two comparisons of triangles for assessing both the numerator and the denominator. A Euclidean distance d was used for the comparison of the continuous variables and serves as our joint descriptor of x_c and y_c. To compute the Euclidean distance, the variables were normalized dividing each value by the maximum value taken by that feature, resulting in variables with values between 0 and 1. Owing to the conditional status $LR_{c|d}$, distances were computed between x_c and y_c only if the discrete variables x_d and y_d corresponded. The distance is defined as follows:

$$d(x_c,y_c) = \Delta^2 A_1 + \Delta^2 L_{1-2} + \Delta^2 A_2 + \Delta^2 L_{2-3} + \Delta^2 A_3 + \Delta^2 L_{3-1}$$

where Δ^2 is the squared difference between the corresponding variables from x and y.

Hence, the LR of interest can be estimated by the ratio of the densities of d obtained under two distinct states S and $\bar{S}$.

$$LR_{c|d} = \frac{p(d|x_d,y_d,S,I)}{p(d|x_d,y_d,\bar{S},I)}$$

These two densities have been estimated, for right loops fingerprints, from feature vectors originating from a common source (within variability) on the one hand, and from different sources on the other (between variability). The estimation of $LR_{c|d}$ is the purpose of the reminder of the paper. The within-variability density is assessed from the pairwise cross comparisons of feature vectors within their family set. The between-variability density is assessed from the pairwise comparisons of the mark feature vector and the feature vectors extracted for the between variability. Both densities have been computed using a kernel smoothing method (built-in *ksdensity* function from Matlab®/Statistics toolbox®, The Mathworks, Inc., Natick, MA). Details about the datasets and the concept of family set are given in the next section.

TABLE 2—*RMED, RMEP, and LRs obtained for configurations of three minutiae for dataset 1.*

			S Is True		$\bar{S}$ Is True	
	RMED (%)	RMEP (%)	$LR_{c\|d}$ Minimum	$LR_{c\|d}$ Maximum	$LR_{c\|d}$ Minimum	$LR_{c\|d}$ Maximum
All zones	2.42	2.62	0.009	2.87×10^3	3.16×10^{-7}	6.53×10^1
Core zone	5.14	1.93	0.01	2.43×10^3	1.13×10^{-7}	4.00×10^2
Delta zone	2.44	3.19	0.025	3.42×10^3	3.19×10^{-7}	4.16×10^3
Left zone	2.32	0.66	0.01	2.57×10^3	1.30×10^{-7}	4.09×10^1
Right zone	1.21	2.85	0.057	3.35×10^3	2.93×10^{-7}	3.60×10^2

RMED, rate of misleading evidence in favor of the defense; RMEP, rate of misleading evidence in favor of the prosecution; LR, likelihood ratio.

TABLE 3—*RMED, RMEP, and LRs obtained for configurations of three minutiae for dataset 2.*

	RMED (%)	RMEP (%)	S Is True		$\bar{S}$ Is True	
			LR_{cld} Minimum	LR_{cld} Maximum	LR_{cld} Minimum	LR_{cld} Maximum
All zones	3.27	3.24	0.01	7.65×10^3	1.94×10^{-7}	2.69×10^2
Core zone	3.74	2.43	0.006	1.99×10^3	5.61×10^{-7}	4.12×10^2
Delta zone	2.39	5.20	0.01	1.60×10^4	1.70×10^{-6}	1.12×10^2
Left zone	3.33	2.38	0.008	2.98×10^3	4.34×10^{-7}	1.03×10^3
Right zone	3.09	1.16	0.05	1.89×10^3	1.09×10^{-6}	1.45×10^3

RMED, rate of misleading evidence in favor of the defense; RMEP, rate of misleading evidence in favor of the prosecution; LR, likelihood ratio.

Acquisition of Data

We will consider separately data informing within finger variability for the numerator of the LR, from data informing the between variability for the denominator of the LR.

Within-Finger Variability

For the description of the within-finger variability of configurations of 3 minutiæ, a dataset of 216 fingerprints from four fingers (all right loops) has been obtained. The fingers used were the middle finger and the thumb of two donors, one male and one female, both donors being roughly of the same age (30s). An optical acquisition method based on coaxial episcopy illumination was used. For the acquisition of different images showing distortion in several directions, the following method has been used. The protocol requires that the donor moves his feet at nine fixed positions, while keeping his finger on the same position on the acquisition device. The closest position (of the nine) between the feet and the acquisition device is of 20 cm. The nine positions of the donor are contained in a square of a side length of 50 cm. The finger is applied on the glass pane and the distortion depends on

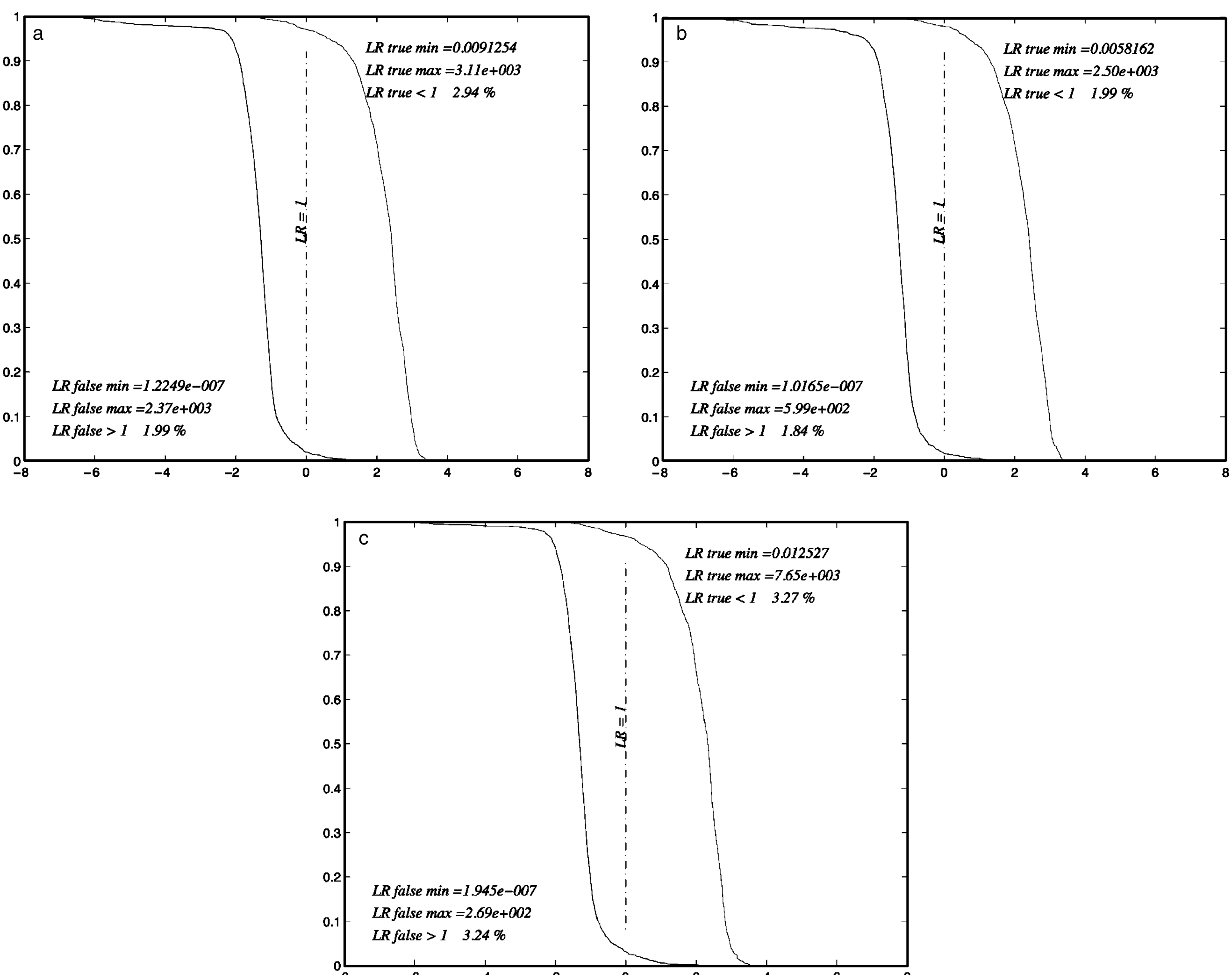

FIG. 10—*Tippett plot of the likelihood ratios over all regions for index (a) and middle (b) fingers in dataset 1 and for thumbs in dataset 2 (c).*

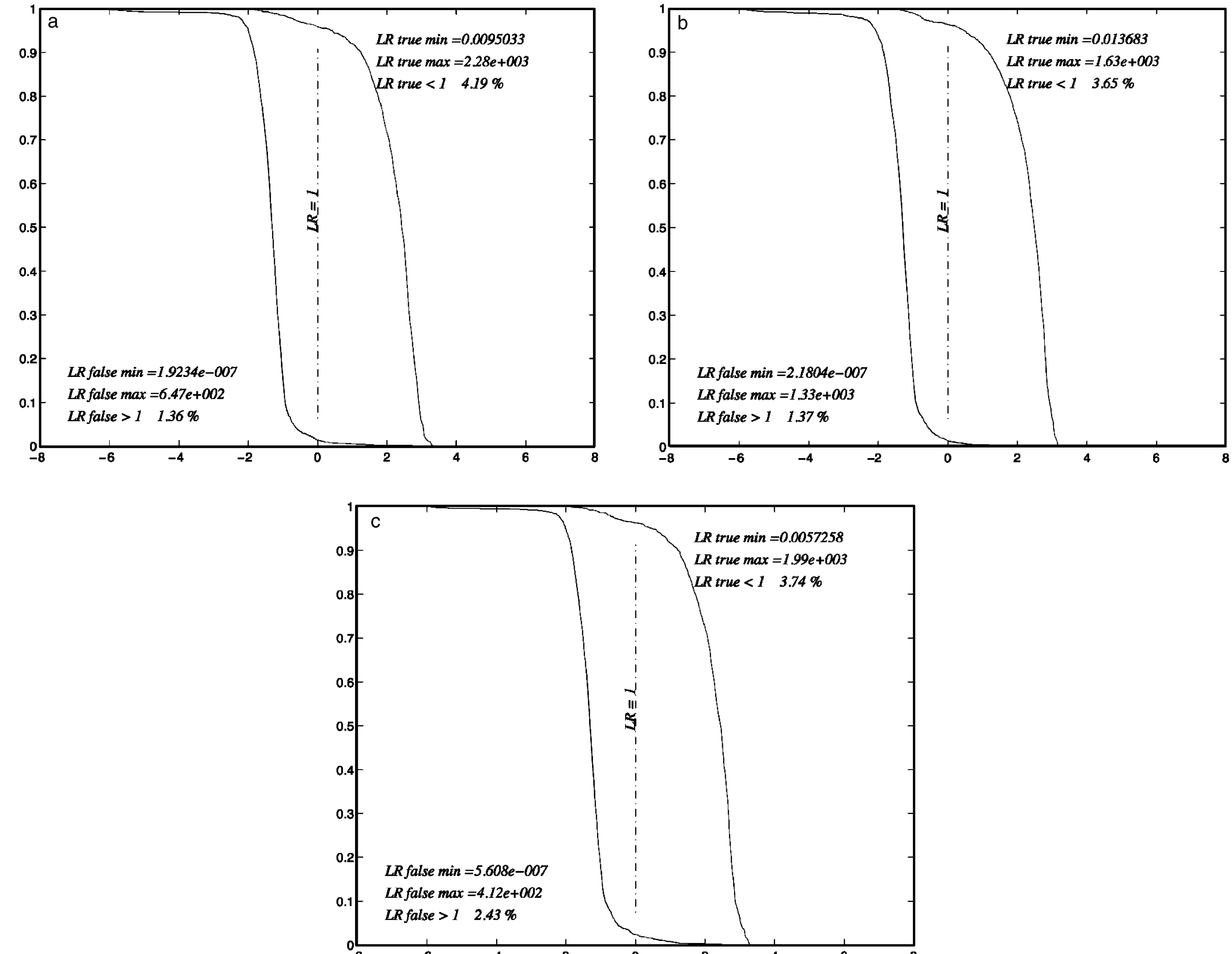

FIG. 11—*Tippett plot of the likelihood ratio in the core region for index (a) and middle (b) fingers in dataset 1 and for thumbs in dataset 2 (c).*

the position of the donor. Image acquisition was performed using a Fuji Finepix S2 Pro® camera, using the maximal interpolated resolution of 4256 × 2848 pixels. An example is given in Fig. 9.

The resulting resolution of the images is *c*. 2500 dpi, and they have been acquired and stored in TIFF (Tagged Image File Format). An image of this quality allows the estimation of within variability due to distortion only. Uncertainty as to the type of minutiæ is not taken into account at this stage.

Each image has been preprocessed according to the procedure described in section 4. In addition, triangles were grouped into family sets. A family set is a set of triangles coming from the same finger and the same set of minutiæ. These families represent the amount of distortion a given configuration can endure. Delaunay triangulation is reproducible on fixed points, but as minutia positions in this setup are not constant (due to distortion), Delaunay triangulation on different images may lead, for the same donor finger, to different triangulation. In order to avoid this and to ensure reproducibility in the triangulation, triangles were manually corrected and attributed, using the corresponding inked triangulated fingerprint as a template. A maximum of 54 triangles can constitute a family set (per prints acquired). However, due to the fact that distortion may reduce the papillary information available, the number of triangles per family set varies between 1 and 54.

Between-Finger Variability

Two datasets are available for the investigation of the between-finger variability. The first—*dataset 1*—has been acquired during a previous study (13); the second—*dataset 2*—has been acquired during this research effort. At this stage, we decided to keep these two datasets separate in order to investigate the effect of a change of population on the LRs.

Fingerprints in dataset 1 are ulnar loops from right index and middle fingers, as shown in Table 1. They originate from a population of 686 randomly selected males registered within the Swiss criminal justice fingerprint database.

Fingerprints in dataset 2 are ulnar loops from right thumb fingers. They originate from a population of 132 randomly selected males registered within the Swiss criminal justice fingerprint database.

The fingerprint images of dataset 1 had been previously digitized (800 dpi, 8 bits depth) binarized, skeletonized, and manually checked against the original grayscale image, in order to correct all artifacts due to the automated binarization and thinning processes. This processing scheme is fully described elsewhere (13). The working set for this study is then composed of the corrected skeletons re-sampled to 500 dpi. The feature vectors were obtained using the procedure described, leading to feature vectors for 90,327 triangles.

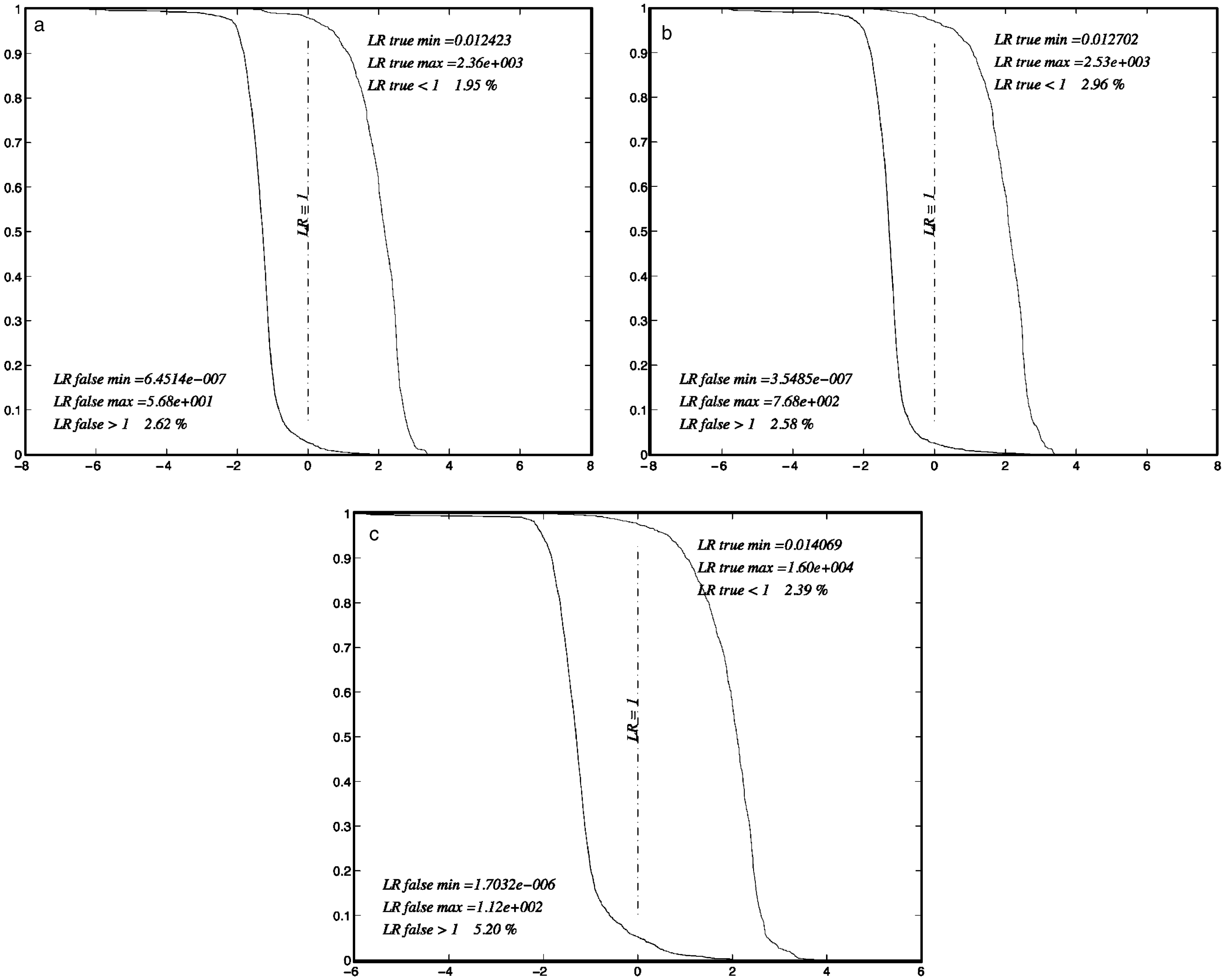

FIG. 12—*Tippett plot of the likelihood ratio in the delta region for index (a) and middle (b) fingers in dataset 1 and for thumbs in dataset 2 (c).*

The images from dataset 2 were acquired in grayscale at a resolution of 800 dpi and processed, for a total of 23,051 triangles.

Results

Our aim is to assess the efficiency of the system using Tippett plots. The Tippett plots were constructed by resampling techniques using the results of 2000 LRs for each hypothesis (4000 LRs in total). To compute $LR_{c|d}$ under S, two "matching" configurations (one considered to be the mark, one considered to be the print) are randomly selected from the families of corresponding triangles coming from the within-donor datasets. To compute the $LR_{c|d}$ under $\bar{S}$, two "nonmatching" configurations are randomly selected from the database made of the configurations constructed from between-sources database. Tests were conducted to ensure the robustness of Tippett plots when computed with a resampling procedure of 2000 LRs under each hypothesis. The originating region of minutia configurations was taken into account to assess the change in expected LRs between core, delta, right, and left periphery. The Tippett plot is a specific representation of the distribution of LRs obtained under both hypotheses. On the x-axis, the $\log_{10}(LR_{c|d})$ is given. On the y-axis, one minus the cumulative distribution (from probability of 1 to 0) of the LRs is given. The Tippett plot then gives one minus the cumulative distribution for, respectively, the LRs computed under S (called *LR true* on the Tippett plot) and the LRs computed under $\bar{S}$ (called *LR false* on the Tippett plot). These plots allow also to study and compare the proportions of misleading evidence: the percentage of $LR_{c|d} < 1$ when the prosecution proposition S is true and percentage of $LR_{c|d} > 1$ when the defense proposition $\bar{S}$ is true. We define these two rates of misleading results as follows:

Rate of misleading evidence in favor of the defense (RMED): among all $LR_{c|d}$ computed under the prosecution proposition S, proportion of $LR_{c|d}$ below 1. On the Tippett plots, this rate is denoted *LR true* < 1.

Rate of misleading evidence in favor of the prosecution (RMEP): among all $LR_{c|d}$ computed under the defense proposition ($\bar{S}$), proportion of $LR_{c|d}$ above 1. On the Tippett plots, this rate is denoted *LR false > 1*.

The results obtained for dataset 1 are summarized in Table 2, and those for dataset 2 are summarized in Table 3.

The Tippett plots are given in Figs. 10–14.

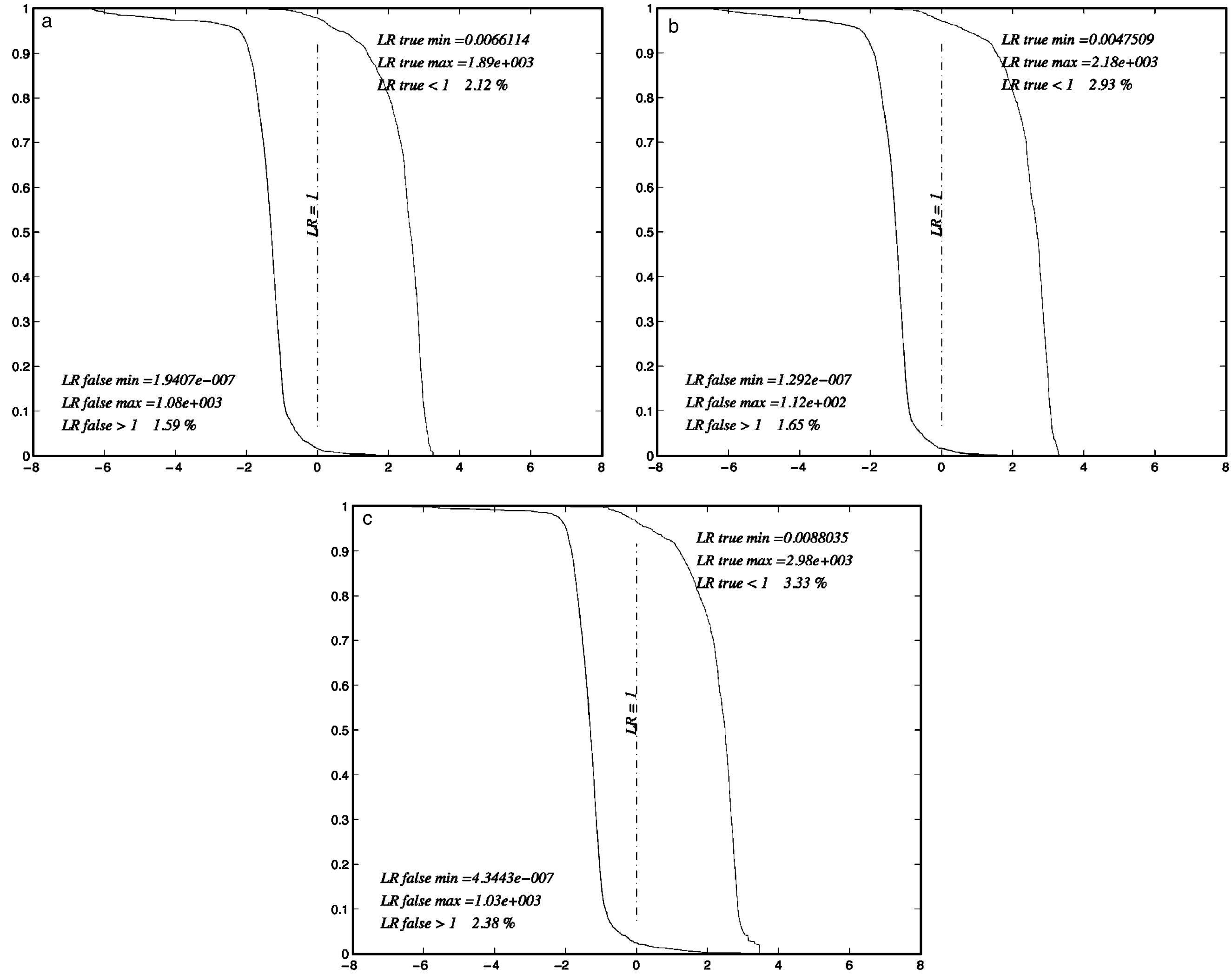

FIG. 13—*Tippett plot of the likelihood ratio in the left periphery for index (a) and middle (b) fingers in dataset 1 and for thumbs in dataset 2 (c).*

In order to verify that for a given triangle the LRs computed are stable to a change in database, a subset of the dataset acquired for the description of within finger variability has been used as a basis for comparison of the LR obtained for a given triangle. This subset contains 219 triangles, which are reproduced a maximum of 36 times. This was done under the defense proposition, $\bar{S}$, as well as under the prosecution proposition S.

As dataset 1 contains far more three-minutiæ configurations coming from right loops than dataset 2, the triangles from the training set have been subsampled to the same number (23,051-triangles). The following figures illustrate these comparisons (Figs. 15 and 16).

The results show that even though the LRs obtained are not linearly correlated, particularly under the prosecution proposition, their logarithms are ($R^2 = 0.974$ and $= 0.945$, respectively). This means that these results correspond in magnitude between the two databases used. Furthermore, no great influence of database size is observed.

Discussion and Conclusion

The results show that the data-driven approach adopted here is robust; the magnitude of LRs obtained under both propositions (S and $\bar{S}$) stresses upon the major evidential contribution that small portions of fingermark (three minutiæ) can provide regardless of their position on the general pattern. The Tippett plots computed for all regions together and separately for each of the different zones show slight differences between them. The comparison between the two datasets through the rates of misleading evidence does not suggest a problem in relation to a change in database.

Of course, focused on three minutiæ only, the present model constitutes a "proof of concept" but it encapsulates important features:

– the weight of evidence is expressed through a LR at the source level that takes into account both within- and between-sample variability;
– the model captures the type of minutiæ, their location, orientation, and relative relationships;
– the computation of LR is heavily based on data both for the numerator and denominator avoiding questionable distributional or independence assumptions; and
– validation has been made through experiments by simulating cases where sources were known. It allowed estimating two decisive rates of misleading evidence (RMED and RMEP). As the value 1 for the LR is used to distinguish the two rates

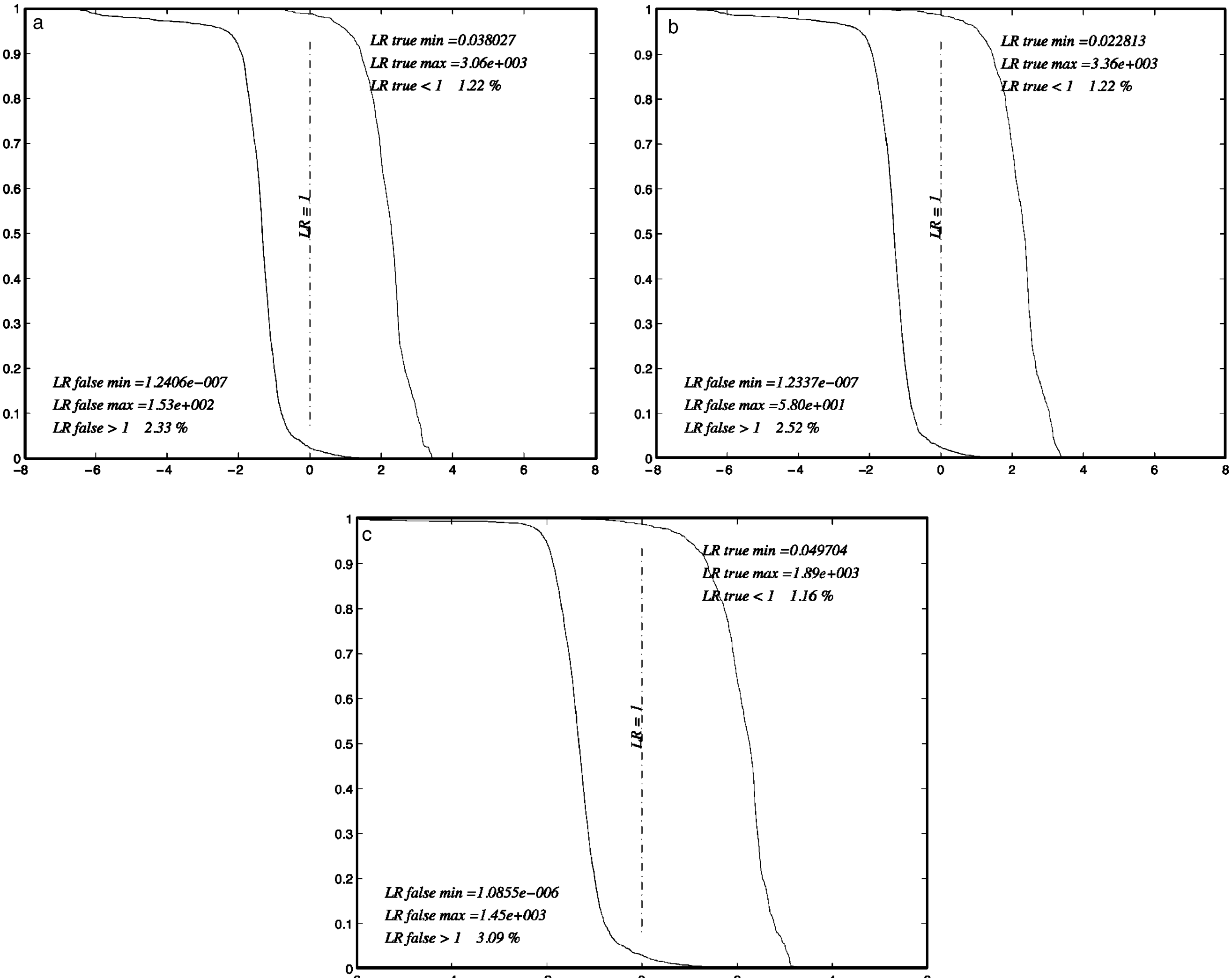

FIG. 14—*Tippett plot of the likelihood ratio in the right periphery for index (a) and middle (b) fingers in dataset 1 and for thumbs in dataset 2 (c).*

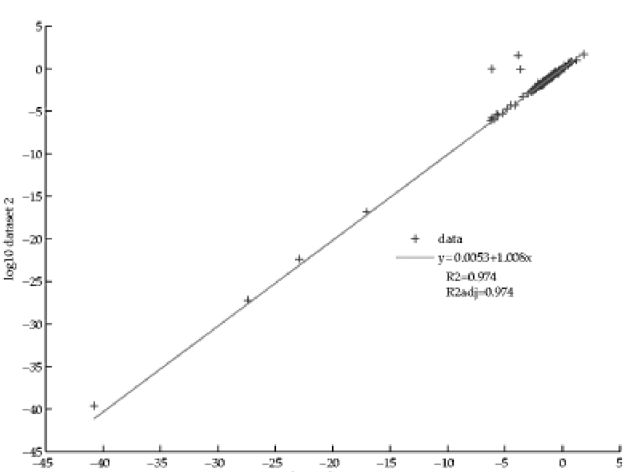

FIG. 15—*Comparison of results for a collection of triangles between dataset 1 and dataset 2 under the defense proposition $\bar{S}$.*

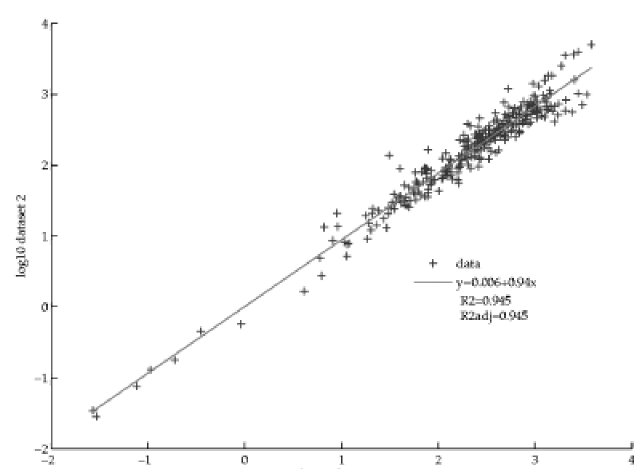

FIG. 16—*Comparison of results for a collection of triangles between dataset 1 and dataset 2 under the prosecution proposition S.*

(RMED and RMEP), by shifting this "threshold" we can adapt a system with a predefined RMED or RMEP. As a policy, we may want to minimize RMEP with the effect of increasing RMED. Such a consideration will have to be taken into account at the time we would deploy an operational system.

It should be emphasized that the LRs that are presented in this work are directly correlated to the feature vectors used. Indeed, these feature vectors are only one possible mathematical representation of the anthropometric reality. Changes in the way fingerprint features are extracted from fingerprints and encoded may result in different LRs. The effect of such changes may be studied by applying the above-described simulations, with the same data sets, on the new model and by comparing the resulting Tippett plots, RMED, and RMEP with the one presented in this research.

Based on these qualities, we envisage expanding this model to deal with more than three minutiæ and to study a larger collection of friction ridge skin impressions.

Acknowledgments

The research is supported by the US Technical Support Working Group contract DAAD05-03-C-0038.

References

1. Epstein R. Fingerprints meet Daubert: the myth of fingerprint "science" is revealed. South Calif Law Rev 2002;75:605–55.
2. Saks MJ. The legal and scientific evaluation of forensic science (especially fingerprint expert testimony). Seton Hall Law Rev 2003;33: 1167–87.
3. Cole SA. Grandfathering evidence: fingerprint admissibility rulings from Jennings to Llera plaza and back again. Am Crim Law Rev 2004; 41:1189–276.
4. Thompson WC, Cole SA. Lessons from the Brandon Mayfield case. The Champion 2005;29:32–4.
5. Zabell SL. Fingerprint evidence. J Law Policy 2005;13:143–79.
6. Saks MJ, Koehler JJ. The coming paradigm shift in forensic identification science. Science 2005;309:892–5.
7. McKie IAJ. There's nane ever fear'd that the truth should be heard but they whom the truth would indite. Sci Justice 2003;43:161–5.
8. Stacey RB. A report on the erroneous fingerprint individualization in the Madrid train bombing case. J Forensic Identification 2004;54:706–18.
9. Cole SA. More than zero: accounting for error in latent fingerprint identification. J Crim Law Criminol 2005;95:985–1078.
10. Budowle B, Buscaglia J, Schwartz Perlman R. Review of the scientific basis for friction ridge skin comparisons as a means of identification: committee findings and recommendations. Forensic Sci Commun 2006;8: http://www.fbi.gov/hq/lab/fsc/current/research/2006_01_research02.htm.
11. Champod C, Lennard CJ, Margot PA, Stoilovic M. Fingerprints and other ridge skin impressions. Boca Raton: CRC Press, 2004.
12. Champod C. Reconnaissance automatique et analyse statistique des minuties sur les empreintes digitales [Ph.D. thesis]. Lausanne, Switzerland: Université de Lausanne, Institut de Police Scientifique et de Criminologie, 1996.
13. Champod C, Margot PA. Computer assisted analysis of minutiæ occurrences on fingerprints. In: Springer E, Almog J, editors. Proceedings of the International Symposium on Fingerprint Detection and Identification; June 26–30, 1995; Ne'urim, Israel. Jerusalem: Israel National Police, 1996: 305–18.
14. Champod C, Margot P. Analysis of minutiæ occurrences in fingerprints – the search for non-combined minutiæ. In: Takatori T, Takasu A, editors. Current topics in Forensic Science – Proceedings of the 14th Meeting of the International Association of Forensic Sciences; August 26–30, 1996. Tokyo: Shunderson Communications, 1997:55–8.
15. Stoney DA. Measurement of fingerprint individuality. In: Lee HC, Gaensslen RE, editors. Advances in fingerprint technology. Boca Raton: CRC Press, 2001:327–87.
16. Royall RM. Statistical evidence – a likelihood paradigm. London: Chapman Hall, 1997.
17. Aitken CGG, Taroni F. Statistics and the evaluation of evidence for forensic scientists. 2nd ed. Chichester: John Wiley and Sons Ltd, 2004.
18. Walsh SJ, Triggs CM, Buckleton JS. Forensic DNA evidence interpretation methods and interpretation. Boca Raton: CRC Press, 2004.
19. Stoney DA. Quantitative assessment of fingerprint individuality [Ph.D. thesis]. Berkeley, USA: University of California, Berkeley, 1985.
20. Champod C. Identification / individualization: overview and meaning of id. In: Siegel J, Saukko P, Knupfer G, editors. Encyclopedia of forensic science. London: Academic Press, 2000:1077–83.
21. Champod C, Evett I, Kuchler B. Earmarks as evidence: a critical review. J Forensic Sci 2001;46:1275–84.
22. Champod C, Evett IW. A probabilistic approach to fingerprint evidence. J Forensic Identification 2001;51:101–22.
23. Evett IW, Buckleton JS. Statistical analysis of STR data. In: Bär W, editor. Advances in forensic haemogenetics. Berlin: Springer Verlag, 1996: 79–86.
24. Meuwly D. Reconnaissance de locuteurs en sciences forensiques: L'apport d'une approche automatique [Ph.D. thesis]. Lausanne, Switzerland: Université de Lausanne, Institut de Police Scientifique et de Criminologie, 2001.
25. Drygajlo A, Meuwly D, Alexander A. Statistical and bayesian interpretation of evidence in forensic automatic speaker recognition. Proceedings of the 8th European Conference on Speech Communication and Technology (Eurospeech - Interspeech 2003); 2003 September 1–4; Geneva, Switzerland. Geneva, Switzerland: The International Speech Communication Association, 2003;689–92.
26. Gonzales-Rodriguez J, Fierrez-Aguilar J, Ramos-Castro D, Ortega-Garcia J. Bayesian analysis of fingerprint, face and signature evidences with automatic biometric systems. Forensic Sci Int 2005;155:126–40.
27. Thai R.. Fingerprint image enhancement and minutiae extraction [M.Sc. thesis]. Crawley, Australia: The University of Western Australia, School of Computer Science and Software Engineering, 2003.
28. Hong L, Wan Y, Jain A. Fingerprint image enhancement: algorithm and performance evaluation. IEEE Trans Pattern Anal Mach Intell 1998; 20: 777–89.
29. Bebis G, Deaconu T, Georgiopoulos M. Fingerprint identification using delaunay triangulation. IEEE International Conference on Information Intelligence and Systems (ICIIS-99); 1999 Oct 31–Nov 3; Rockville, Maryland. Washington DC: IEEE Computer Society, 1999; 452–9.
30. Kovacs-Vajna ZM. A fingerprint verification system based on triangular matching and dynamic time wraping. IEEE Trans Pattern Anal Mach Intell 2000;22:1266–76.
31. Cappelli R, Lumini A, Maio D, Maltoni D. Fingerprint classification by directional image partitioning. IEEE Trans Pattern Anal Mach Intell 1999;21:402–21.

Additional information and reprint requests:
Christophe Champod, Ph.D.
Ecole des Sciences Criminelles
Institut de Police Scientifique
Batochime, Quartier Sorge
Université de Lausanne
CH-1015 Lausanne-Dorigny
Switzerland
E-mail: cchampod@unil.ch